MULTIPLICITY OF CHARGED PARTICLES IN π^- NEON INTERACTIONS AT 25 AND 50 GeV/c*

By B. S. Yuldashev**, T. H. Burnett***, H. J. Lubatti, K. Moriyasu, H. Rudnicka**** and A. Wróblewski*****

Visual Techniques Laboratory, Department of Physics, University of Washington, Seattle Washington 98195

The multiplicity distributions of charged particles produced in π^- Ne interactions at 25 and 50 GeV/c are presented and compared with π nucleus and π nucleon data. It is found that for the produced negative particles, the dependence of the dispersion on the average multiplicity is compatible with that observed for $\pi^{\pm}p$ and $\pi^{\pm}d$ interactions. We observe that the average multiplicity of produced negatives, $\langle N^{Pr} \rangle$, is correlated with the number of observed protons, N_p, and obtain an effective target mass $m_{eff} \simeq (N_p+1)m_p$.

1. Introduction

In this paper we present results on the multiplicities of secondaries produced in π^- Ne interactions at 25 and 50 GeV/c. The experiment is performed in the FNAL 15-foot bubble chamber filled with a neon-hydrogen mixture. The large volume of the 15-foot chamber makes it possible for the secondary particles to separate which enhances the probability of determining correctly the multiplicity of the charged secondaries. In addition, the bubble chamber allows us to observe "slow" particles and identify the protons from ionization. Thus, the correlations between the number of observed protons and the fast secondary particles can be studied.

While there have been considerable data available for hadron-nucleus interactions at high energies, much have come from emulsion experiments where either the sample of events is small or the target is a composite of several different nuclei with significantly different atomic weights. This latter point has made it difficult to study the dependence

of multiplicity on the atomic number of the nucleus. High-statistics electronic experiments have studied interactions on solid targets; however, in those experiments, it is not possible to measure the slow protons which are produced in conjunction with the fast secondaries. Experiments in bubble chambers with heavy mixtures have the advantage of 4π-geometry, a unique target, and the possibility of detecting the slow protons. Moreover, the fast secondaries can be separated according to charge and a good efficiency for detecting neutral particles such as γ's and V^0's is intrinsic to the device. Thus, corrections can be made for neutral particles which materialize close to the interaction vertex and bias the determination of the charge multiplicity.

In Section 2 we present the experimental details and procedures. The results and a discussion of the results are given in Section 3 and 4, respectively, and the summary and conclusions are presented in Section 5.

2. Experimental procedure

The data were obtained from an exposure of the Fermilab 15-foot bubble chamber filled with a heavy mixture of $Ne-H_2$ (64% atomic neon) to 25 and 50 GeV/c π^- beams. The radiation and interaction lengths for this liquid are 39 cm and 1.4 m, respectively.

The film was scanned for all interactions within the fiducial volume. This resulted in the 444 events at 25 GeV/c and 956 events at 50 GeV/c which are analyzed in this paper. The number of positive (minimum ionizing), N_+, and negative, N_-, secondary tracks were recorded. Also the number of identifiable protons, N_p, was recorded for each event.

Proton tracks can be identified visually by ionization and range in the momentum interval $160 \lesssim p \lesssim 800$ MeV/c, which corresponds to track lengths $0.15 \lesssim l \lesssim 75$ cm. Thus, protons with momenta $p \gtrsim 800$ MeV/c are included in the N_+ sample. All identified Dalitz-pairs, close γ's ($\lesssim 1$ cm), δ-electrons, and close secondary interactions were recorded. These were used to correct statistically the average multiplicities. One-prong events were detected only for laboratory scattering angles $\theta_{lab} \gtrsim 2°$. Since most of the coherent elastic π^-Ne interactions have $\theta_{lab} \ll 2°$ only a very small fraction of the elastic π^-Ne events contribute to the one-prong events.

In order to study π^-Ne interactions we must remove the background of π^-p interactions on free hydrogen. This is done statistically using the cross sections for π^-Ne[1] and π^-p [2] collisions and the measured multiplicity distributions of charged particles in π^-p interactions at 25 and 50 GeV/c [3, 4]. We estimate that $37 \pm 8\%$ of the elastic π^-p events are lost because of very short recoil protons. Thus, using inelastic cross sections $\sigma(\pi^-Ne) = (273 \pm 6)$ mb and $\sigma(\pi^-Ne) = (268 \pm 6)$ mb for visible π^-Ne interactions at 25 and 50 GeV/c [1], respectively, we concluded that only $8.5\% \pm 2.0\%$ of the recorded events were π^-p interactions on free protons, and this amount is subtracted from the observed multiplicity distributions.

After making the above corrections there are still some biases in our data. The 0- and 1-charged particle topologies have scanning biases which are difficult to correct. In

---

[1] Interpolated from the data of Ref. [1].

addition, events in which there is only one "fast" negative particle include both quasi--elastic scattering of the incident pion with the bound (quasi-free) nucleon in the neon nucleus and inelastic interactions. Since we wish to compare the π^-Ne charged particle multiplicity distribution with that observed in π^-p inelastic interactions (i. e., to compare production of particles on free nucleons with bound nucleons in the nuclear environment), it will be necessary to either correct our observed $N_- = 1$ sample or to compare only for $N_- \geqslant 2$, i.e., when there is at least one negative particle produced in the interaction, $N_-^{Pr} \geqslant 1$. We stress that previous experiments have not made this distinction. A further discussion will be given in Section 3.

3. Results

The multiplicity distributions of the fast charged, $N_\pm = N_+ + N_-$, and negative, N_-, particles are given in Table I (a, b) and shown in Fig. 1 (a, b). In Table I we also give an estimate of the coherent π^-Ne contribution obtained by extrapolating the measured
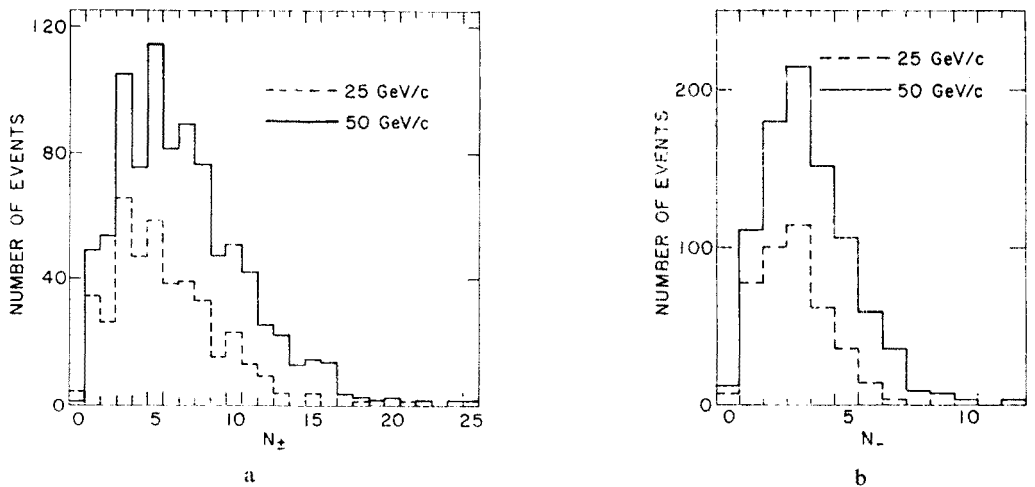

Fig. 1. Multiplicity distributions for π^-Ne interactions at 25 GeV/c (dashed) and 50 GeV/c (solid):
(a) Positive and negative particles as defined in the text and (b) negative particles only

$\sigma_{coh}/A^{2/3}$ cross sections to these energies [5, 6]. The statistical isospin model [7] is used to estimate the contribution of coherent channels with neutral pions. The total $N_\pm$ distribution is shown in Fig. 1a, where we observe an excess of events at odd multiplicities extending to $N_\pm = 7$. The same phenomenon was observed in π^-Ne interactions at 10.5 and 205 GeV/c [8] and was interpreted as the result of diffractive dissociation of the incident π^-. If we assume that the excess of events in $N_\pm = 3, 5$ and 7 originates from diffractive dissociation (including coherent π^-Ne channels), then we obtain 22 ± 7 mb and 24 ± 5 mb for π^- diffractive dissociation at 25 and 50 GeV/c, respectively. These values are comparable with the

Multiplicity distributions — all charged particles

$N_{\pm}$	25 GeV/c		50 GeV/c	
	Observed	π^-Ne [a]	Observed	π^-Ne [a]
0	5	4.8 ±2.2	1	0.7±0.7
1	38	34.8 ±5.9 (4.7) [b]	54	49.0±7.0 (12.7) [b]
2	30	25.7 ±5.1	59	53.4± 7.3
3	69	65.7 ±8.1 (7.0)	112	105.7±10.3 (19.0)
4	57	46.8 ±6.8	90	75.7± 8.7
5	60	57.7 ±7.6 (0.6)	120	114.2±10.7 (2.0)
6	45	38.0 ±6.2	94	80.9± 9.0
7	40	39.0 ±6.2	93	89.1± 9.4
8	36	33.1 ±5.8	85	76.1± 8.7
9	15	14.7 ±3.8	49	47.3± 6.9
10	23	22.3 ±4.7	55	51.2± 7.2
11	10	9.95±3.1	43	42.3± 6.5
12	8	7.9 ±2.8	27	25.4± 5.0
13	3	3.0 ±1.7	23	22.9± 4.8
14	—	—	13	12.7± 3.4
15	3	3.0 ±1.7	14	14.0± 3.7
16	—	—	13	13.0± 3.6
17	—	—	3	3.0± 1.7
18	1	1.0 ±1.0	2	2.0± 1.4
19	—	—	1	1.0± 1.0
20	—	...	2	2.0± 1.4
21	1	1.0 ±1.0	—	—
22			1	1.0± 1.0
23			—	—
24			1	1.0± 1.0
25			1	1.0± 1.0
$\sum$	444	408.5	956	884.6

[a] Corrected for π^-p events. [b] Estimated contribution of coherent channels.

diffractive dissociation cross sections of 17.2 ± 3.0 mb and 23.4 ± 3.0 mb observed in π^-Ne interactions at 10.5 and 205 GeV/c, respectively [8].

In Fig. 2 we present the multiplicity distribution of the negative particles in π^-Ne interactions at 25 and 50 GeV/c using the KNO scaling variables [9]. (Note that we include $N_- = 0, 1$ in $\langle N_-\rangle$.) We have also included in Fig. 2 data for π^-Ne interactions at 10.5 [10], π^-C interactions from 4 to 40 GeV/c [11], and π^-p interactions at 50 GeV/c (solid line) [4]. The scaled multiplicity distributions are in reasonable agreement with each other and consistent with KNO scaling for π^--nucleus interactions. The average multiplicity and dispersion, $D_- = [\langle N_-^2\rangle - \langle N_-\rangle^2]^{1/2}$, of σ_{N_-} are given in Table II.

Multiplicity distributions — negatives only

N_-	25 GeV/c		50 GeV/c	
	Observed	π^-Ne [a]	Observed	π^-Ne [a]
0	7	6.8± 2.6	11	10.7± 3.3
1	84	76.5± 8.7 (4.7) [b]	122	110.4±10.5 (12.7) [b]
2	112	98.5±10.0 (7.0)	201	180.4±13.4 (19.0)
3	123	113.7±10.7 (0.6)	230	212.1±14.6 (2.0)
4	65	61.1± 7.8	164	151.2±12.3
5	37	36.1± 6.0	111	105.5±10.3
6	14	13.8± 3.7	61	58.7± 7.7
7	2	2.0± 1.4	37	36.6± 6.0
8			9	9.0± 3.0
9			7	7.0± 2.6
10			2	2.0± 1.4
11			—	—
12			1	1.0± 1.0
$\sum$	444	408.5	956	884.6

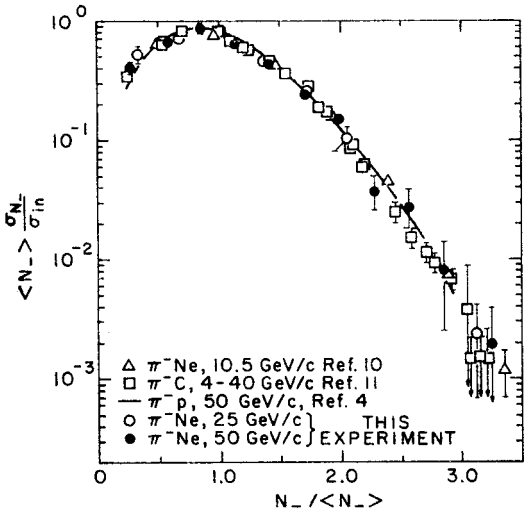[a] Corrected for π^-p events. [b] Estimated contribution of coherent channels.

Fig. 2. Distribution of KNO scaling variables. π^-p and other π^- Nucleus data are plotted for comparison

Figure 3 presents the dispersion of the multiplicity distributions of negative particles as a function of the average multiplicity of π^-Ne interactions for incident momenta from 10.5 to 50 GeV/c. We have also plotted similar data for π^-C collisions [11]. At fit of these data to $D_- = A_- + B_- \langle N_- \rangle$ yields $A_- = -0.05 \pm 0.03$ and $B_- = 0.53 \pm 0.02$. The fitted

TABLE II

Average multiplicities and dispersions

	25 GeV/c	50 GeV/c
$\langle N_- \rangle$	2.91 ± 0.07	3.51 ± 0.07
D_-	1.46 ± 0.11	1.74 ± 0.08
$\langle N_-^{Pr} \rangle$ [a]	2.27 ± 0.06	2.85 ± 0.07
D_-^{Pr}	1.19 ± 0.09	1.63 ± 0.08

[a] $\langle N_-^{Pr} \rangle = \sum\limits_{N_-=2} (N_- - 1)\, \sigma_{N_-} \Big/ \sum\limits_{N_-=2} \sigma_{N_-}.$

slope B_- is similar to that obtained in $\pi^- p$ interactions [12]. It is clear from Fig. 3 that $\langle N_- \rangle / D_-$ for π^- nucleus interactions is systematically lower than that obtained for $\pi^- p$ interactions. However, as discussed in Section 2, the events with $N_- = 1$ in π^- nucleus interactions can result from quasi-elastic (incoherent) interactions with no production of
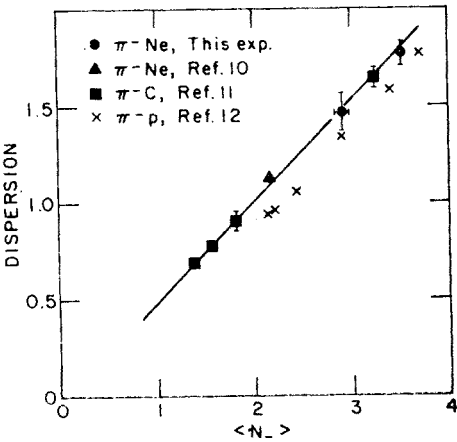

Fig. 3. Comparison of dispersion versus N_- for πp and π nucleus data. Solid line is a fit to $D_- = A_- + B\langle N_- \rangle$ with $A = -0.05 \pm 0.03$ and $B = 0.53 \pm 0.02$

new particles but only, perhaps, nuclear fragments. Since there is no unique way to estimate the contribution of such processes, we consider only events with $N_-^{Pr} \geqslant 1$ ($N_- \geqslant 2$). Thus calculated $\langle N_-^{Pr} \rangle$, D_-^{Pr} values are given in Table II. In Fig. 4 we give the D_-^{Pr} vs $\langle N_-^{Pr} \rangle$ dependence for these data. For comparison, we also give $\pi^- p$ and $\pi^- d$ values [12]. These data all fall on the same curve, consistent with the universality of the dependence of dispersion on average multiplicity of produced negative particles for hadron-nucleus and hadron-nucleon interactions. We stress that the difference between $\pi^- p$ and π^--nucleus data shown in Fig. 3 results from having included the $N_- = 1$ channel which contains, for the π^-nucleus interactions, the quasi elastic $\pi^- p$ scattering, while the $\pi^- p$ data with which we compare contains only inelastic interactions.
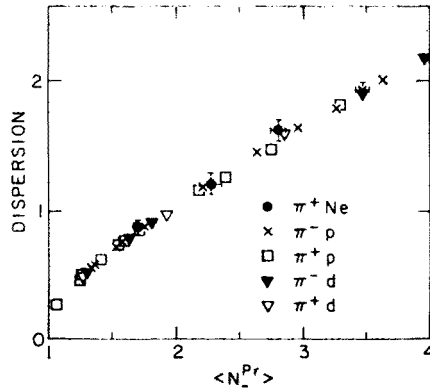
Fig. 4. Comparison of dispersion versus number of produced negative particles for π^- Ne (this experiment and Ref. [10]), $\pi^\pm$ d and $\pi^\pm$ p (Ref. [12])

The multiplicity distributions of the identified protons, N_p, observed at 25 and 50 GeV/c are shown in Fig. 5 where it can be seen that, within the statistical errors, there is no energy dependence. Thus, the multiplicity distributions of protons with momenta $160 \lesssim p \lesssim 800$ MeV/c exhibits a "scaling"-like behavior which also has been observed for
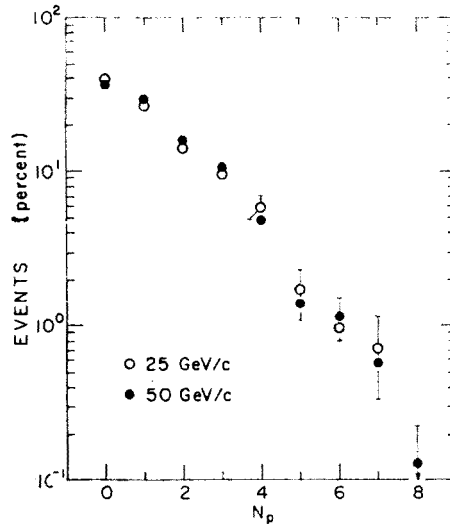

Fig. 5. Fraction of events with identified protons

π^- Carbon interactions [11, 13] and for collisions of pions and protons with emulsion nuclei [14]. This can be understood qualitatively as a consequence of an approximate energy independence of the distribution of the number of inelastic collisions in the nucleus.

The average multiplicities of identified protons at 25 and 50 GeV are $\langle N_p \rangle = 1.32 \pm 0.07$ and $\langle N_p \rangle = 1.37 \pm 0.05$, respectively. In π^-C interactions between 4 and 40 GeV/c

$\langle N_{\mathrm{p}}\rangle = 0.97\pm0.02$ and is independent of energy [13]. Taking $\langle N_{\mathrm{p}}\rangle$ to be energy independent and assuming $\langle N_{\mathrm{p}}\rangle \sim A^{\alpha}$ we obtain from the Ne/C comparison $\alpha = 0.63\pm0.09$. This suggests that $\langle N_{\mathrm{p}}\rangle$ has an $A^{2/3}$ rather than the $A^{1/3}$ dependence expected by some models of hadron-nucleus interactions (see, e. g. Refs [15, 16]), which may indicate some rescattering contributions.

4. Discussion

To compare our data with theoretical models, we begin with the most basic measurement, the average multiplicity. For reasons explained above, we consider only N_{-}^{Pr}. Assuming that the ratio of N^{Pr} to the total multiplicity (including neutrals) is the same for neon and hydrogen, we divide $\langle N_{-}^{\mathrm{Pr}}\rangle$ by the equivalent value for πp scattering as a measure of the quantity $R_A = \langle N\rangle_{\pi A}/\langle N\rangle_{\pi p}$. For 25 and 50 GeV we obtain 1.19 ± 0.03 and 1.20 ± 0.03, respectively.

Comparing our experimental values for R_A with theoretical predictions is complicated by the fact that three of the models, the energy flux cascade model of Gottfried [15], the two-phase model of Fishbane and Trefil [16], and the parton model approach of Brodsky, Gunion and Kühn (BGK) [17], require specification of $\langle \nu\rangle$, the average number of collisions in the nucleus, which cannot be unambiguously determined. For these models, we calculate two values for R_A, based on two reasonable parametrization of $\langle\nu\rangle$: (1) $\nu_1 = A\sigma_{hN}/\sigma_{hA}$ [19], where σ_{hN} and σ_{hA} are hadron-nucleon and -nucleus inelastic cross sections. Using measured cross sections [1, 2] we find 1.52 and 1.55 for ν_1 at 25 and 50 GeV, respectively; (2) $\nu_2 = \sum_{\nu} \nu\sigma(\nu)/\sum_{\nu} \sigma(\nu)$ in which the cross section for ν collisions, $\sigma(\nu)$, is obtained using the Glauber formalism [20] with $\sigma_{\pi N} = 20$ mb and a Gaussian nuclear density. This gives $\nu_2 = 1.67$ for πNe. To apply the model of BGK, the fraction of particles produced in the fragmentation regions also must be specified. We have chosen 100%, appropriate for low energies where no plateau exists[2]. In this case, the prediction coincides with that of

TABLE III

R_A for π^-Ne — experiment and theory

	25 GeV/c	50 GeV/c
Experiment, using N_{-}^{Pr}	1.19 ± 0.03	1.20 ± 0.03
Gottfried [15]	1.17, 1.22[a]	1.18, 1.22
Fishbane and Trefil [16] } BGK [17] }	1.26, 1.33	1.28, 1.33
Nikolaev [18]	1.23	1.27
CTM [22]	1.14	1.14

[a] Values for ν_1 and ν_2, respectively.

[2] At 200 GeV/c lab momentum, the authors choose 20%; if we had used this value, we would have obtained $R_A = 1.30$ and 1.41 for ν_1 and ν_2, respectively.

Fishbane and Trefil. Predictions of the above models for R_A at 25 and 50 GeV, and for v_1 and v_2, are shown in Table III.

Also in Table III are predictions of the intranuclear cascading parton model of Nikolaev [18] and the Collective Tube Model (CTM) of Dar et al. [22]. Values for the former were obtained by interpolation from a figure in Ref. [18] and we calculated the latter using the $\sigma(v)$ partial cross sections employed to calculate v_2.

Considering uncertainties in applying the models, including the ambiguity in determining $\langle v \rangle$, it appears that none of the models disagrees enough with the data to be ruled out.

In this experiment, protons with momenta $\gtrsim 800$ MeV/c are not identified during the scanning and are included among the N_+ particles. Evidence for these protons comes from the net charge $Q = N_+ - N_-$ of the fast particles. In Fig. 6a, b we plot the average value of
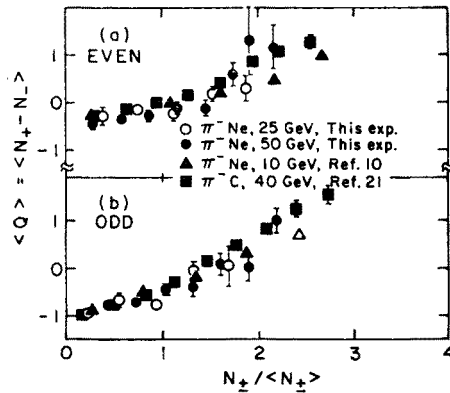

Fig. 6. Comparison of the dependence of the net charge on the number of charged tracks ($N_\pm$): (a) $N_\pm$ even; (b) $N_\pm$ odd

Q, for each multiplicity $N_\pm$. The scaled multiplicity $N_\pm/\langle N_\pm \rangle$ is used in order to compare these data with two other experiments [10, 21]. It may be concluded from Fig. 6 that the dependence of $\langle Q \rangle$ versus $N_\pm/\langle N_\pm \rangle$ is similar for all three experiments. The total number of protons emitted in $\pi^\pm$Ne interactions at 10.5 GeV/c was determined by employing charge symmetry to be 1.3 times larger than the number of visually identified protons [10]. The similarity of the $\langle Q \rangle$ vs $N_\pm/\langle N_\pm \rangle$ distributions (Fig. 6) suggests a similar proportion of fast protons in this experiment.

Multiple proton production is characteristic of hadron-nucleus scattering and suggests that several nucleons were involved in the interaction. Since all models that describe the behavior of a hadron within the nucleus predict that the multiplicity increases with the number of struck nucleons, we show the dependence of $\langle N_-^{pr} \rangle$ on the number of observed protons in Fig. 7a. Similar results have been obtained by Yeager et al. [10] at 10 GeV/c.

In an attempt to quantitatively understand the apparent correlation, we have used the basic assumption of the CTM [22], which is that multiplicity is a function only of the

center-of-mass energy of the beam and a "coherent tube" of nucleons forming a target of N_{eff} nucleons. Thus we use the known dependence of $\langle N_-^{Pr}\rangle$ in π^-p collisions on the center-of-mass energy to obtain an effective target mass[3], m_{eff}, from $s_{eff} = m_\pi^2 + m_{eff}^2 + 2m_{eff}E$.
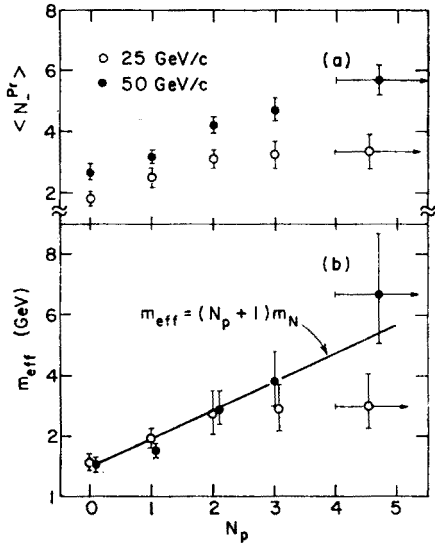

Fig. 7. Dependence of (a) $\langle N_-^{Pr}\rangle$ for $N_-^{Pr} \geqslant 1$ and (b) the effective target mass on the number of visually identified protons, N_p. The solid line represents $m_{eff} = (N_p+1)m_p$

TABLE IV

Effective target masses inferred from multiplicity

N_p	m_{eff} (GeV/c^2)	
	25 GeV/c	50 GeV/c
0 [a]	$1.29^{+0.19}_{-0.17}$	$1.18^{+0.15}_{-0.14}$
1	$1.89^{+0.33}_{-0.29}$	$1.44^{+0.19}_{-0.17}$
2	$2.74^{+0.80}_{-0.64}$	$2.97^{+0.58}_{-0.49}$
3	$2.91^{+0.92}_{-0.71}$	$3.84^{+0.97}_{-0.79}$
$\geqslant 4$	$3.01^{+1.09}_{-0.70}$	$6.73^{+2.03}_{-1.61}$
All events	$1.84^{+0.15}_{-0.13}$	$1.93^{+0.14}_{-0.12}$

[a] Coherent events removed.

[3] We assume that $\langle N_-^{Pr}\rangle$ has the same dependence on s_{eff} as is observed for $\langle N_-^{Pr}\rangle$ versus s in π^-p collisions, i.e., $\langle N_-^{Pr}\rangle = A + B\ln s + C\ln^2 s$, where $A = 0.28\pm0.07$, $B = 0.535\pm0.065$ and $C = 0.025\pm0.010$. We also have used another parametrization for $\langle N_-^{Pr}\rangle$, that is $\langle N_-^{Pr}\rangle = A + B\log p_{LAB}$ and obtained essentially the same results for m_{eff}.

The values obtained for each N_p are given in Table IV and shown in Fig. 7b, where it can be seen that the data are consistent with $m_{eff} = N_{eff}\, m_p$, where $N_{eff} = N_p + 1$. The CTM in fact predicts such a linear dependence.

In order to make a more detailed check of this prediction, we have selected the statistically largest sample of events at 50 GeV/c with $N_p = 2$ (corresponding to $N_{eff} = 3.16 + {}^{+0.61}_{-0.52}$) and $N_-^{Pr} \geqslant 1$ and compared the multiplicity distribution, $\varrho(N_-^{Pr}) = \varrho_{N_-^{Pr}}/(\sum \sigma_{N_-^{Pr}})$, with that observed for π^-p collisions at 100 GeV/c [23] (corresponding to $N_{eff} \simeq 2$) and 147 GeV/c
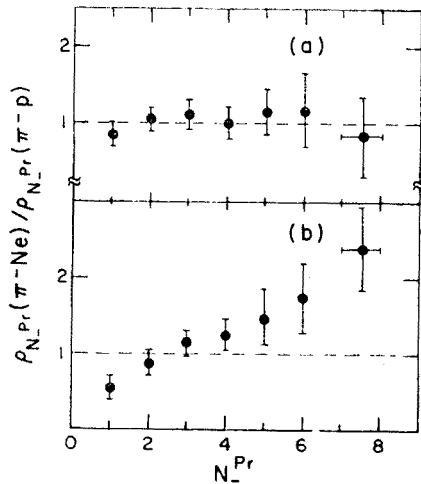

Fig. 8. The ratio of the multiplicity distributions of negative particles for π^-Ne interactions with $N_p = 2$ at 50 GeV/c to π^-p interactions at (a) 147 GeV [24] and (b) 100 GeV/c [23]

[24] (corresponding to $N_{eff} \simeq 3$). The results are shown in Figs. 8a, b. It is seen that, consistent with the CTM predictions, the $\varrho(N_-^{Pr})$ distribution for events with $N = 2$ is in good agreement with the 147 GeV/c data (Fig. 8a); however, it is not compatible with the 100 GeV/c data (Fig. 8b).

5. Conclusions

We have presented data on the multiplicity of particles in π^-Ne collisions at 25 and 50 GeV/c. The multiplicity distribution of negative particles was found to obey nuclear KNO scaling. Because of the contamination of quasi-elastic scattering, the dependence of D_- on $\langle N_- \rangle$ in π^--nucleus collisions differs from that in π^-p collisions. However, if we consider produced negative particles, N_-^{Pr}, then the π^--nucleus and π^-p data have the same D_-^{Pr} vs $\langle N_-^{Pr} \rangle$ dependence. We have examined the predictions of several models for R_A and found none in serious disagreement with the experimental values. Comparing the average number of protons with momentum $160 \lesssim p \lesssim 800$ MeV/c produced in π^-C and π^-Ne collisions we conclude that $\langle N_p \rangle \propto A^{2/3}$.

We also have observed that the average multiplicity of produced negative particles, $\langle N^{Pr}_- \rangle$, increases with the number of observed protons, N_p. By using the observed $\langle N^{Pr}_- \rangle$ dependence on center-of-mass energy squared, s, we obtained an effective target mass for each value of N_p. Within errors, this was found to be consistent with $m_{eff} = (N_p + 1)m_p$ and in agreement with the expectations of the coherent tube model.

REFERENCES

[1] J. C. Allaby et al., *Sov. J. Nucl. Phys.* **12**, 295 (1971).

[2] E. Bracci et al., CERN/HERA 72-1 (1972).

[3] J. W. Elbert et al., *Nucl. Phys.* **B19**, 85 (1970).

[4] G. A. Akopdjanov et al., *Nucl. Phys.* **B75**, 401 (1974).

[5] V. G. Grishin et al., *Sov. J. Nucl. Phys.* **14**, 712 (1972).

[6] N. Angelov et al., *Sov. J. Nucl. Phys.* **24**, 186 (1976).

[7] F. Cerulus, *Nuovo Cimento* **19**, 529 (1961).

[8] J. R. Elliott et al., *Phys. Rev. Lett.* **34**, 607 (1975).

[9] Z. Koba, H. B. Nielsen, P. Olesen, *Nucl. Phys.* **B40**, 317 (1970).

[10] W. M. Yeager et al., *Phys. Rev.* **D16**, 1294 (1977).

[11] S. A. Azimov et al., *Nucl. Phys.* **B107**, 45 (1976).

[12] A. Wróblewski, Proceedings of VIII International Symposium on Multiparticle Reactions, Kayserberg 1977; *Acta Phys. Pol.* **B4**, 857 (1973).

[13] S. A. Azimov et al., *Sov. J. Nucl. Phys.* **22**, 608 (1975).

[14] See, for example, E. M. Friedlander, A. Friedman, *Nuovo Cimento* **52A**, 912 (1967); K. G. Gulamov, Proceedings of the International Conference on High Energy Physics and Nuclear Structure, Zurich 1977.

[15] K. Gottfried, *High Energy Physics and Nuclear Structure*, Ed. G. Tibell, North-Holland 1973, p. 79.

[16] P. M. Fishbane, J. S. Trefil, *Phys. Lett.* **51B**, 139 (1974).

[17] S. J. Brodsky, J. F. Gunion, J. H. Kühn, *Phys. Rev. Lett.* **39**, 1120 (1977).

[18] N. N. Nikolaev, Preprint Landau Institute of Theoretical Physics, ITP-18 (1975).

[19] O. V. Kancheli, *JETP Lett.* **18**, 274 (1973).

[20] P. M. Fishbane, J. S. Trefil, *Phys. Rev.* **D9**, 168 (1974).

[21] N. Angelov et al., *Yad. Fiz.* **25**, 1009 (1977) and JINR Preprint Pl-10324, Dubna 1976.

[22] G. Berlad, A. Dar, G. Eilam, *Phys. Rev.* **D13**, 161 (1976).

[23] E. L. Berger et al., *Nucl. Phys.* **B77**, 365 (1974).

[24] D. G. Fong et al., *Phys. Lett.* **53B**, 290 (1974).